Chapter 6

Transcriptomics analysis of Escaper and Multi-Omics analysis of -mouse, golden retriever models and DMD patient data points to glycolytic defect

INTRODUCTION

As seen in previous chapters, DMD disease progression includes many aberrations of metabolism, signaling pathways, calcium imbalance, oxidative stress, inflammatory overdrive, and immune cell infiltration, making it irreversible. Without clear cause-effect relations between the pathological processes associated with DMD disease, multi-omics studies can be a source of essential pathways targeted for therapy. The multi-omics on the *mdx* model recently found pathways of metabolism, and it was revealed that ECM composition has been most affected (Van Pelt et al., 2021). The weighted gene co-expression analysis of transcriptomics data found immune pathways enriched in DMD patients (Wei et al., 2022). This approach has found that pyruvate accumulation is the primary cause of Amyotrophic Lateral Sclerosis (ALS) (Sai Swaroop et al., 2022) which was not previously thought to be a pathology initiator.

We tried to compare the transcriptomics data for "Escaper" GRMD available online (Vieira et al., 2015), to find new mitigated pathways helpful in understanding the rescue mechanism. The proteomics or metabolomic data for "Escaper" GRMD is not available. Hence, the multi-omics approach was used on other publicly available *mdx,* GRMD, and DMD patients' databases to find commonly enriched pathways across these three organisms.

MATERIALS AND METHODS

The GEO ID for the data analyzed is as follows. The Escaper is transcriptomic GSE69040. Other GRMD muscle is transcriptomic ID GSE68626. The *mdx* data ID is GSE64418. The patient IDs used were GSE1004, GSE-1007, and GSE-109178. The proteomics data from Capitanio et al., (2020) was used for analysis. The patient-derived metabolites data from Sharma et al., (2003), Srivastava et al., (2018), and Dabaj et al., (2020) were used as the latter contained previously reported GRMD and *mdx* data.

WORKFLOW

All the transcriptomics data was analyzed using the online GEO2R web tool. The differentially expressed genes (DEGs) list was downloaded. The DEGs were considered significant when the p-value was less than or equal to 0.05, and there was a 2-fold change (increase or decrease). Significant DEGs names/symbols for GRMDs were identified using the *bioDBnet* online tool from Agilent/Affymetrix IDs available on the GEO platform for given data. Significant DEG lists from each transcriptomic data were separately used for pathway enrichment analysis with the *Enrichr* online tool. The KEGG pathways generated by *Enrichr* were selected based on the significance ($p \leq 0.05$) and arranged according to "Combined Scores" as it considers false discovery rate (FDR) also. The best 10-15 pathways based on combined scores were used for finding commonly enriched pathways. Ven diagram for common pathways was created using *Venny2.0* online tool. The proteomics data for DMD patients from Capitanio et al., (2020) article was similarly used with *Enrichr*. The pathways with the top combined scores were selected. The names of metabolites were fed into "*MetaboAnalyst"* to find KEGG and SMPDB-based pathway enrichment, where pathways with FDR less than 0.25 were selected. Metabolite data for GRMD could not be analyzed because the *MetaboAnalyst* platform does not have tools for this organism. The common pathways between transcriptomics, proteomics, and metabolomics were similarly collected and represented using the Venny2.0 tool as diagrams and tables.

RESULTS

KEGG PATHWAY ENRICHMENT FOUND PATHWAYS ENRICHED SPECIFICALLY IN THE ESCAPER.

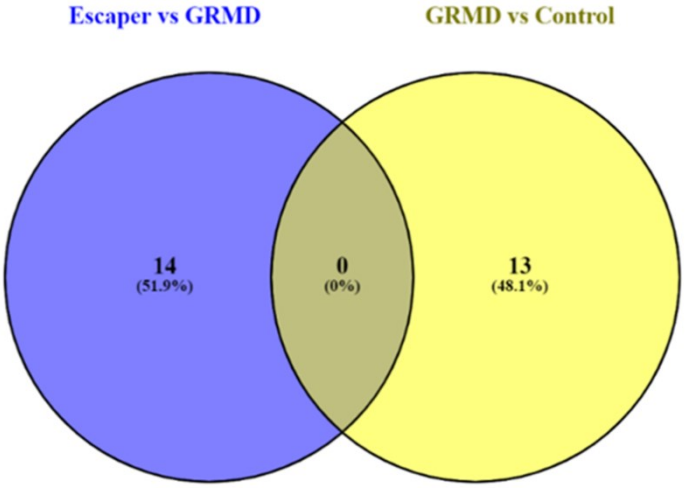

Figure 6.1: Venn diagram represents the commonly enriched pathway between Escaper dogs vs GRMD dogs and GRMD dogs vs Control dogs.

Table 6.1: Escaper vs. GRMD common pathways enriched during transcriptomic analysis

Sr. No.	Pathways	Genes
1.	Caffeine metabolism	NAT2
2.	Phenylalanine, tyrosine, and tryptophan biosynthesis	GOT1
3.	Sulfur metabolism	BPNT1
4.	Circadian rhythm	BHLHE40; PRKAB1
5.	Proteasome	PSMD7; PSMA2
6.	Phenylalanine metabolism	GOT1
7.	Sphingolipid metabolism	SGPL1; KDSR
8.	Vascular smooth muscle contraction	ACTA2; ADORA2A; NPR1; PRKACB
9.	Parkinson disease	PSMD7; ADORA2A; PSMA2; NDUFC1; PRKACB; EIF2S1
10.	Spinocerebellar ataxia	PSMD7; PSMA2; ATXN1L; PUM2
11.	Regulation of lipolysis in adipocytes	NPR1; PRKACB
12.	Aldosterone synthesis and secretion	NPR1; DAGLB; PRKACB
13.	Arginine biosynthesis	GOT1
14.	Terpenoid backbone biosynthesis	IDI1

Table 6.2 : GRMD vs. Control common pathways enriched during transcriptomic analysis

Sr. No.	Pathways	Genes
1.	Citrate cycle (TCA cycle)	MDH1; DLAT; SDHD; SDHA;DLD; IDH3A
2.	Glyoxylate and dicarboxylate metabolism	GCSH; MDH1; MMUT; DLD; ACAT1
3.	Synthesis and degradation of ketone bodies	HMGCS1; ACAT1
4.	Pentose phosphate pathway	ALDOB; PFKM; PGM1; FBP2
5.	Glycolysis / Gluconeogenesis	DLAT; ALDOB; DLD; PFKM; PGM1; FBP2
6.	Glycine, serine, and threonine metabolism	GCSH; GATM; MAOB; DLD
7.	Pyruvate metabolism	MDH1; DLAT; DLD; ACAT1
8.	Valine, leucine and isoleucine degradation	HMGCS1; MMUT; DLD; ACAT1
9.	Fructose and mannose metabolism	ALDOB; PFKM; FBP2
10.	Propanoate metabolism	MMUT; DLD; ACAT1
11.	Pantothenate and CoA biosynthesis	PANK3; GADL1
12.	Oxidative phosphorylation	NDUFA8; ATP6V1G2; NDUFB10;COX17;SDHD;CYC1; SDHA
13.	Histidine metabolism	MAOB; CARNMT1

Table 6.3: Pathways enriched exclusive to Escaper dogs

Eleven elements include exclusively in "Escaper vs. GRMD"	
1.	Sulphur metabolism
2.	Circadian rhythm
3.	Proteasome
4.	Phenylalanine metabolism
5.	Sphingolipid metabolism
6.	Vascular Smooth Muscle Contraction
7.	Parkinson disease
8.	Spinocerebellar ataxia
9.	Regulation of lipolysis in adipocytes
10.	Aldosterone synthesis and secretion
11.	Arginine biosynthesis

The WIKI pathways-based enrichment was also initially done but did not reveal pathways with enrichment that have $p \leq 0.05$ for significance. The KEGG pathway enrichment, as Figure 6.1 shows metabolic pathways common between Affected and Escaper GRMD compared to Control. Table 6.1 lists pathways enriched in Escaper vs. Affected, while Table 6.2 lists pathways enriched in Escaper vs. Control. Table 6.3 shows a pathway list unique to only Escaper, related to amino acids and lipid metabolism in "Escapers." Another interesting pathway is proteasomal degradation, as it is known to cause excess atrophy in DMD. It is also important to note that pathways scoring high in affected GRMD compared to healthy, like glyoxylate and dicarboxylate, glycolysis, and tricarboxylic acid metabolism, are absent in the escapers.

This is a single transcriptomic data from a single rescue report for DMD. In order to observe how disease-associated pathways from the above study compared to overall DMD disease, other reported data from GRMD, patients, and mouse models of DMD were analyzed from the publicly available GEO database.

The WIKI pathway enrichment did not yield any common pathways even within the same study with the same platform for human DMD patient transcriptomics data (Figure 6.2). Hence, KEGG pathway enrichment was considered for the rest of the studies. Similarly, using *MetaboAnalyst*, the metabolite list from Dabaj et al., (2020) found only 2 KEGG pathways with

FDR less than 0.25. The metabolite list from Sharma et al., (2003) found only 2 SMPDB pathways with FDR less than 0.25. It is important to mention that all three-metabolite data used here showed "arginine metabolism" as a significant pathway in both SMPDB and KEGG-based enrichment (unpublished data from our lab). The methods and data which generated more pathways of significance were considered. The datasets that generated unique pathways were not considered further as the aim is to find common pathways. As apparent from figures 6.4 and 6.5, Arginine metabolism appears in human proteomics data and common metabolomic pathways between humans and mice. Though glyoxylate and dicarboxylate pathway is the only common element between transcriptomics data of human, *mdx*, and GRMD in dystrophic conditions (Figure 6.3), the other pathways common between human and *mdx*, GRMD, and *mdx* were also taken for other typical pathway building.

WIKIBASED PATHWAY ENRICHMENT FOR PATIENT TRANSCRIPTOMICS DATA

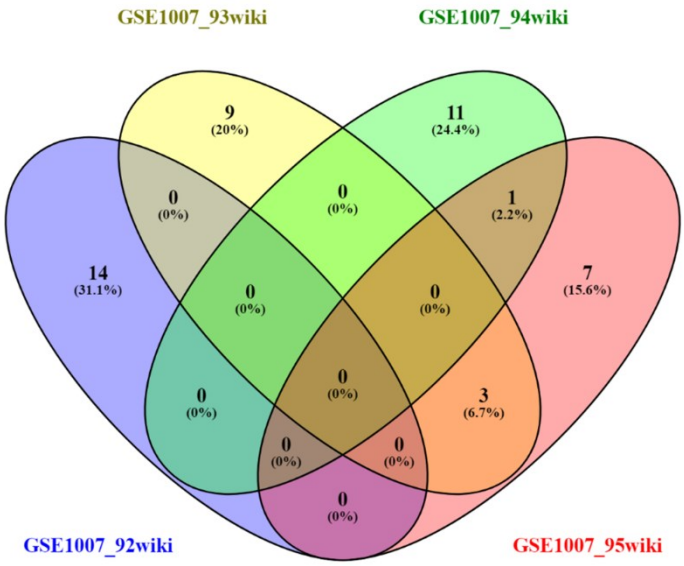

Figure 6.2: Venn diagram represents that the WIKI based enriched pathway for human DMD patient transcriptomics data.

The wiki pathways-based enrichment did not find any common pathways even within the same geo-platform for human transcriptomics data.

THE COMMON KEGG-ENRICHED PATHWAYS BETWEEN HUMAN, GRMD AND *MDX* TRANSCRIPTOMICS DATA

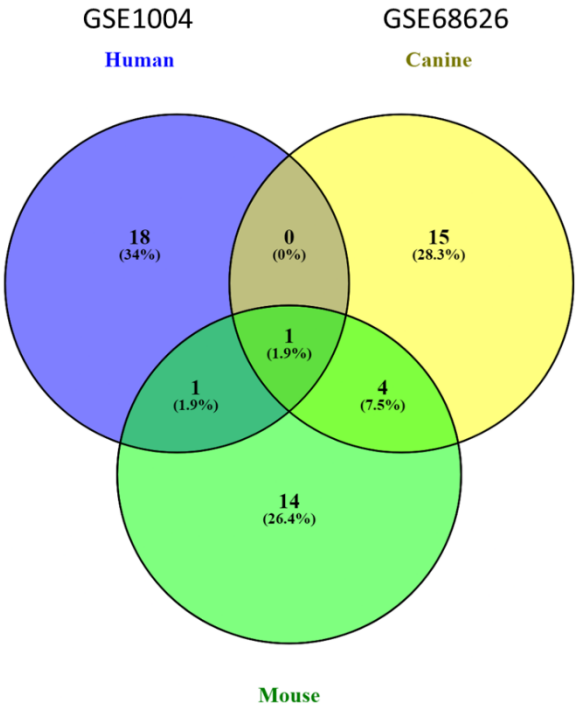

KEGG Pathways

Names	total	elements
Canine Human Mice	1	GLYOXYLATE AND DICARBOXYLATE METABOLISM
Human Mice	1	CIRCADIAN RHYTHM
Canine Mice	4	SYNTHESIS AND DEGRADATION OF KETONE BODIES
		GLYCOLYSIS / GLUCONEOGENESIS
		PYRUVATE METABOLISM
		PROPANOATE METABOLISM

Figure 6.3: Venn diagram shows the common KEGG-enriched pathways between Human patients, GRMD dogs and *mdx* mouse transcriptomics data.

PROTEOMICS-BASED PATHWAY ENRICHMENT POINTS TO DEFECTS IN GLUCOSE METABOLISM AND EXTRACELLULAR MATRIX CHANGES

Table 6.4: Proteomics based KEGG pathway enrichment of patient samples

Sr. No.	Term	Combined Score	Genes
1.	Citrate cycle (TCA cycle)	1371.7435	PDHA1; SUCLA2; MDH1; MDH2; OGDH; ACO2; SDHA
2.	Phenylalanine, tyrosine and tryptophan biosynthesis	745.43404	GOT1; GOT2
3.	Glycolysis / Gluconeogenesis	544.72766	TPI1; PDHA1; ADH1B; PGAM2; AKR1A1; PGK1; ALDOA; ENO3
4.	Pyruvate metabolism	452.36947	PDHA1; MDH1; ADH1B; MDH2; AKR1A1; ACAT1
5.	Glyoxylate and dicarboxylate metabolism	326.78373	MDH1; MDH2; ACO2; ACAT1
6.	Complement and coagulation cascades	180.98583	C4B; C3; SERPINA1; FGG; A2M; CLU
7.	ECM-receptor interaction	171.41604	COL1A1; COL2A1; COL1A2; COL6A2; COL6A1; COL6A3
8.	Cysteine and methionine metabolism	149.87651	GOT1; MDH1; MDH2; GOT2
9.	Phenylalanine metabolism	143.45595	GOT1; GOT2
10.	Fructose and mannose metabolism	140.00883	TPI1; AKR1B1; ALDOA
11.	Protein digestion and absorption	133.70381	COL1A1; COL1A2; COL2A1; COL6A2; COL6A1; COL6A3
12.	Diabetic cardiomyopathy	127.37933	COL1A1; PDHA1; COL1A2; NDUFA4; VDAC1; UQCRC2; CYC1; SDHA; SLC25A4
13.	Tyrosine metabolism	122.74824	GOT1; ADH1B; GOT2
14.	Cardiac muscle contraction	110.22156	MYL4; ACTC1; MYL3; UQCRC2; CYC1
15.	Arginine biosynthesis	97.770868	GOT1; GOT2
16.	Fat digestion and absorption	93.709132	GOT2; APOA1; ACAT1
17.	HIF-1 signaling pathway	76.832273	TF; PDHA1; PGK1; ALDOA; ENO3
18.	Arginine and proline metabolism	4.364624	CKM; GOT1; GOT2
19.	Cholesterol metabolism	74.364624	APOH; APOA1; VDAC1

METABOLOMICS-BASED KEGG PATHWAY ENRICHMENT FROM HUMAN/PATIENT SAMPLES.

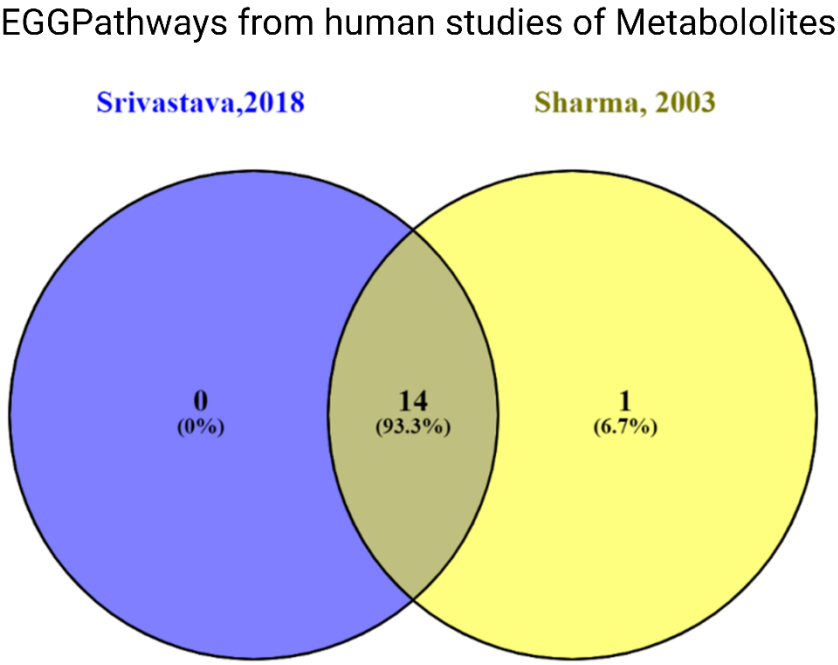

14 common elements in "Srivastava_2018" and "Sharma_2003":
Aminoacyl-tRNA biosynthesis
Alanine, aspartate and glutamate metabolism
Arginine biosynthesis
Pyruvate metabolism
Nitrogen metabolism
D-Glutamine and D-glutamate metabolism
Glycolysis / Gluconeogenesis
Valine, leucine and isoleucine biosynthesis
Glyoxylate and dicarboxylate metabolism
Arginine and proline metabolism
Butanoate metabolism
Histidine metabolism
Citrate cycle (TCA cycle)
Propanoate metabolism

Figure 6.4: Venn diagram shows the Metabolomics-based KEGG enriched pathways From Human/Patient Samples

THE SMPDB PATHWAY ENRICHMENT OF METABOLOMICS STUDIES FOUND MORE COMMON PATHWAYS BETWEEN HUMAN AND *MDX* MOUSE MODELS.

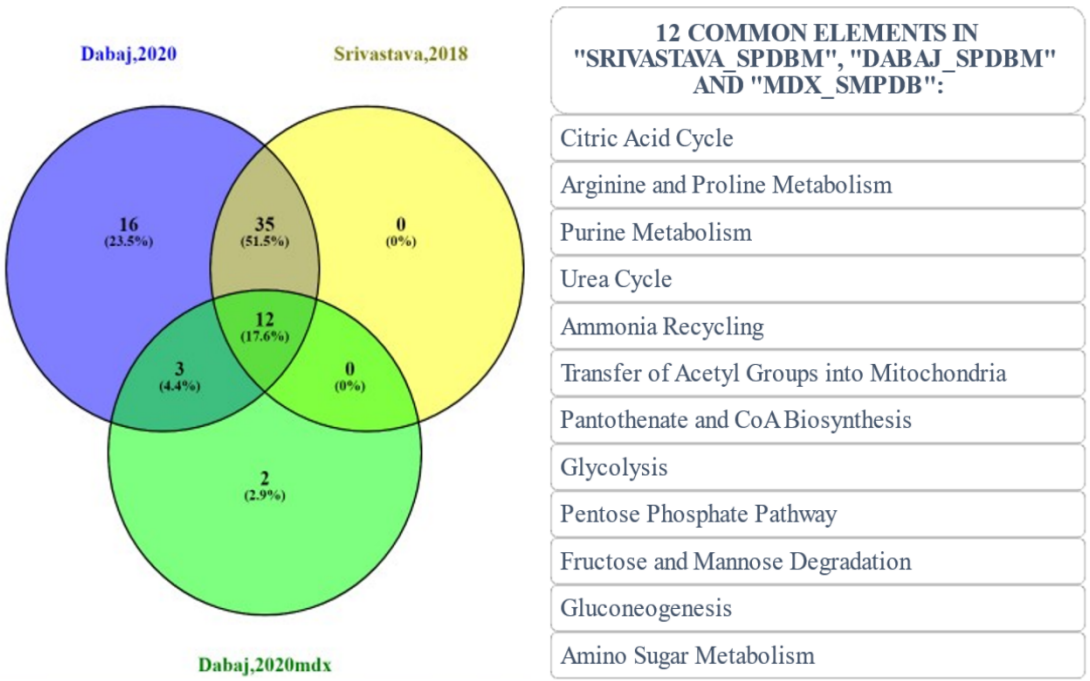

Figure 6.5: Venn diagram shows the SMPDB pathway enriched metabolomics studies between Human and *mdx* mouse models.

COMMON PATHWAYS BETWEEN 3 SPECIES TRANSCRIPTOMICS, HUMAN PROTEOMICS AND HUMAN METABOLOMICS

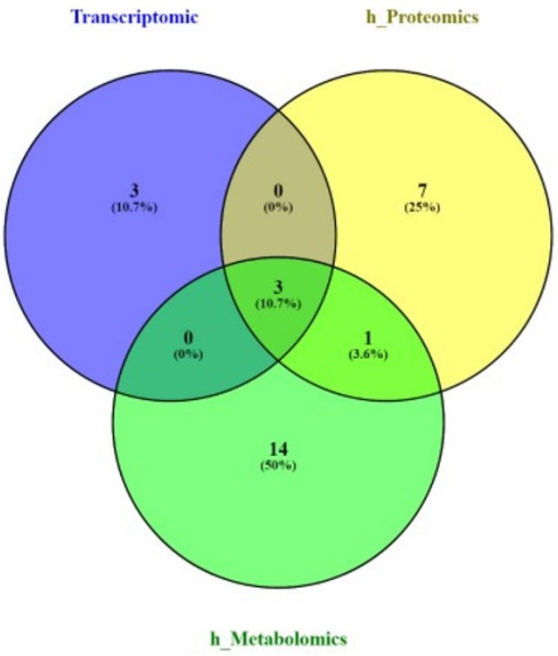

Names	Total	Elements
Transcriptomics, Proteomics, Metabolomics	3	GLYOXYLATE AND DICARBOXYLATE METABOLISM GLYCOLYSIS/ GLUCONEOGENESIS PYRUVATE METABOLISM
Proteomics, Metabolomics	1	CYTRIC ACID CYCLE (TCA)

Figure 6.6: Venn diagram represents the common pathways found between Transcriptomics, Human Proteomics and Human Metabolomics data.

The proteomics data from Capitanio et al., (2020) also points to dysregulated metabolism and changes to ECM and complement pathways of the immune system. The diabetic cardiomyopathy pathway has similar collagen changes to ECM and mitochondrial VDAC and ETC-associated NDUFA4, a part of the NADH Dehydrogenase (Ubiquinone) complex. The TCA cycle (Citric Acid Cycle) is common in Proteomics and Metabolomics pathway enrichment (Figure 6.6). Surprisingly Glyoxylate pathway has come up common between three species transcriptomics, human proteomics, and two species metabolomics-based pathway enrichment. In the *mdx* model, the glyoxylate pathway was scored very low though GRMD and patient data are at the top. Although indirect evidence suggests its involvement in dystrophic pathology, it has never been considered a significant contributor to pathology.

DISCUSSION

The glyoxylates and dicarboxylates are the toxic byproducts of glycolysis, non-enzymatically generated during hyperglycemic conditions. The three carbon products of fructose 1,6 bisphosphate breakdown – dihydroxyacetone phosphate (DHAP) and glyceraldehyde 3 phosphate (GAP) are considered significant sources of glyoxylates. In addition, excess amino acid and fatty acid catabolism end products also can generate glyoxylates (Lange et al., 2012). The Glyoxylates are highly reactive chemical species that react with proteins, and nucleic acids (DNA and RNA), and lipids in the membrane to cause lesions and permeability. The toxic nucleic acid, lipid, protein products of glyoxal reactions are collectively called Advance Glycation End products (AGEs). The ubiquitously expressed Glyoxalase-1 (GLO1) and GLO2 enzymes which, in tandem reactions, convert glyoxal and methylglyoxal (MG) into D-Lactate in a glutathione (reduction) dependent manner form the first line of defense (Thornalley, 1993). GLO1 activity was low in DMD patients, though GLO2 activity remained unchanged (Kar & Pearson, 1975). In addition to GLO enzymes, a family of aldehyde reductases comprising roughly 40 understudied enzymes also contributes to detoxification. AGEs with lipid pore/lesion forming ability quickly enter general circulation from the tissue of formation and bind to receptors on various cells receptor for AGEs - called RAGE (or AGER) (Chavakis et al., 2004).

The excess AGEs production during aging has been shown to cause plasma membrane lesions, ROS production, Ion channel disturbances, increased fibrosis, muscle stiffness, and mitochondrial oxidative stress (Olson et al., 2021), all involved in the pathogenesis of DMD. RAGEs are expressed during embryonic developmental stages but are downregulated in most

tissues postnatally except some tissue-resident stem cells, leukocytes, and lung epithelial lining. RAGE is upregulated in leukocytes and myofibers from dystrophic conditions. The other ligands for RAGE, proteins HMGB1, and S100B, are also upregulated in DMD conditions (Riuzzi et al., 2017; Sagheddu et al., 2018). The knockdown of RAGE reduced pathology progression in *mdx* mice but did not inhibit pathology initiation (Sagheddu et al., 2018). This suggests that AGEs production might be responsible for the excessive inflammatory response in this disease. The myoblasts also express these receptors (RAGE), which might be overactivated due to high ligands accumulation in dystrophic muscles contributing to compromised regeneration. The inhibitors of the RAGE receptor as well as ligands HMGB1 and S100B are under consideration for the development of therapy, but standard glucocorticoid treatment is already known to downregulate the RAGE receptors (Hathout et al., 2019). The natural compound Gingerol from Ginger has been shown to quench the AGEs (Zhu et al., 2015), which has also shown functional rescue in a zebrafish model of DMD at 8-10 dpf but not beyond that and was unable to improve lifespan (Licitra et al., 2021).

All these studies suggest that receptors for AGEs (RAGE) might be involved in the amplification of dystrophic pathology but not initiation. The defects of glycolysis might be more involved in pathology initiation (Nesari et al., 2023) as the initial phase of muscle contraction depends on glycolysis for ATP and metabolite production when energy stores are quickly depleted when mitochondria are still reaching maximum capacity. The elegant radiolabeling study suggested that glucose from glycogenolysis-glycolysis is shunted to glycerol-3-phosphate (G3P) instead of pyruvate and lactic acid (Ellis, 1980), which could be due to the low activity of GPD2 enzyme that reconverts G3P into DHAP which can reenter glycolysis via isomerase (GPI) conversion to GAP. However, this would require the coordination of enzymes involved in the upper and lower half of glycolysis with the glycerol-phosphate shuttle. The discord would increase the toxic glyoxal production on the one hand, whereas, on the other hand, it reduces ATP and pyruvate production from glycolysis. The pyruvate has been shown to activate the GLO1 enzyme (Scott et al., 2017). Hence, lower pyruvate from glycogenolysis-glycolysis during muscle contraction can result in lower defense against glyoxal toxicity. Though the heart and the brain have higher basal glycolysis, it further increases during a sudden increase in workload in the heart (Depre et al., 1999) and neuronal activity in the brain (Vaishnavi et al., 2010). Hence, the absence of dystrophin would affect these two tissues to lesser extents except during excess workload. The overall energy starvation and fold glycolytic requirement between skeletal muscle, heart, and brain would change the

intensity and progression of pathology in the absence of dystrophin, as seen in DMD. As seen in Escaper transcriptomics data, the metabolic rewiring that reduces energy starvation and mitigates glyoxal toxicity could change the disease outcome. The exact mechanism of how Jagged 1 overexpression results in metabolic rewiring needs further study.